Modular polyoxometalate-layered double hydroxides as efficient heterogeneous sulfoxidation and epoxidation catalysts

Tengfei Li,[a†] Wei Zhang,[a†] Wei Chen,[a] Haralampos N. Miras*[b] and Yu-Fei Song*[ac]

Abstract: Selective sulfoxidation of sulfides and epoxidation of olefins are two types of important organic reactions and the corresponding products of sulfoxides, sulfones and epoxides are widely used as raw materials in industrial processes. The fabrication of one efficient catalyst for both reactions, remains a challenging task. In this paper, we report the preparation of a highly efficient heterogeneous catalyst of Mg_3Al-ILs-La$(PW_{11})_2$ using an exfoliation/assembly approach. The catalyst was characterized by FT-IR, XRD, TG/DTA, BET, XPS, ^{29}Si CP/MAS NMR, the ^{27}Al-MAS NMR, SEM, HRTEM, EDX *etc*. The designed catalyst showed high efficiency and selectivity for sulfoxidation of sulphides and epoxidation of olefins under mild conditions at a production rate of 208 mmol g^{-1} h^{-1} and 31 mmol g^{-1} h^{-1}, respectively. Moreover, the Mg_3Al-ILs-La$(PW_{11})_2$ can be recycled and reused at least 5 times without obvious decrease of its catalytic activity. The scaled-up experiments revealed that the catalyst retained its efficiency and robustness, demonstrating the catalyts' great potential for industrial applications.

Introduction

Polyoxometalates (POMs) are a class of molecular metal oxide anions, often incorporating V, Mo, W, or Nb etc., in their highest oxidation states.[1-4] The remarkable properties of POMs such as redox potential, electron-transfer properties, thermal and oxidative stability, acidity, etc., can be finely tuned by incorporation of appropriate addenda metal ions and/or counterions, which endow superior catalytic performance in numerous industrial processes.[5-8] However, the industrial application of POM-based homogeneous catalytic systems has been restricted mainly due to poor separation ability, decomposition issues, environmental concerns, and its high operational cost. Consequently, design of POM-based advanced heterogeneous catalysts has long been and will continue to be the focus for a potentially alternative way to overcome the above limitations and to tune the POM-based material's functionality.

The solidification and immobilization are the two main techniques that have been widely adopted for POM-based heterogeneous catalysts[9-10] such as the incorporation of POMs into porous inorganic supports (silica,[11-12] zeolite,[13] Al_2O_3[14] etc.). However, the immobilization on the aforementioned inorganic supports is usually accompanied by a series of issues which compromise the performance of the designed catalytic systems such as hydrolytic and thermal stability under oxidative conditions; poor mass transfer and accessibility of the active centres; catalyst leaching issues.[10,15] These inherent limitations prevent the development of efficient catalytic systems with desirable functionality and specifications. Thus, it is of fundamental importance to explore appropriate preparation methodologies that will allow the design of efficient, recyclable, stable, and environmentally benign heterogeneous catalytic systems for various industrial applications.

Layered double hydroxides (LDHs) or hydrotalcite-like compounds are a large family of two-dimensional (2D) anionic clays with the general formula $[M_{1-x}^{2+}M_x^{3+}(OH)_2]^{x+}[Ax/n]n\cdot\cdot mH_2O$, where M^{2+} and M^{3+} are di- and trivalent metal cations and [A] are inorganic or organic charge-compensating anions located in the interlayer galleries.[16-17] Each hydroxyl group in the LDH layers is oriented towards the interlayer region forming a network of hydrogen bonds to the interlayer anions and water molecules.[18] LDHs provide a flexible and modular confined space which can be modified by varying the size and the structure of guest molecules. Intercalation of catalytically active species into the interlayer galleries to generate host-guest supramolecular intercalation structures with desirable physical and chemical properties has been proven to be an elegant approach for improving the stability and recyclability of the catalytic system. However, the poor mass transfer of the organic substrates within the interlayer galleries and effective interaction with the active centres of the intercalated catalysts is a major challenge that needs to be taken into careful consideration.

Ionic liquids (ILs) have been extensively investigated as novel green solvents or alternative catalytic materials, which are currently receiving keen interest owing to their unique properties, such as negligible volatility and remarkable solubility.[19-21]

Based on the above considerations, we demonstrate a successful preparation of a novel heterogeneous catalyst of Mg_3Al-ILs-La$(PW_{11})_2$ by intercalation the designed catalytically active POMs into the ILs covalently modified LDHs. Catalytic tests indicate that the designed catalyst Mg_3Al-ILs-La$(PW_{11})_2$ exhibits excellent activity for selective sulfoxidation of sulfides and epoxidation of olefins under mild conditions, coupled with easy recovery and steady reuse.

[a] *T. Li,[†] W. Zhang,[†] W. Chen and Prof. Y.-F.Song**
State Key Laboratory of Chemical Resource Engineering,
Beijing University of Chemical Technology,Beijing 100029, P. R. China.
Email: songyufei@hotmail.com or songyf@mail.buct.edu.cn
[b] Dr. H. N. Miras*
WestCHEM, School of Chemistry
University of Glasgow
Glasgow, G12 8QQ, UK
Email: harism@chem.gla.ac.uk
[c] *Prof. Y.-F.Song**
Beijing Advanced Innovation Center for Soft Matter Science and Engineering, Beijing University of Chemical Technology, Beijing, P. R. China.
[†] *These authors contributed equally to this work*

Supporting information for this article is available on the WWW under http://dx.doi,org/10.xxxxxxxxxx

Results and Discussion

Structural characterization

As shown in Fig. 1a, FT-IR spectrum of $La(PW_{11})_2$ exhibits characteristic peaks centred at 1093, 950, 882 and 769 cm^{-1}, which can be attributed to the asymmetric and symmetric vibrations of W-O_t, asymmetric vibration of W-O_c-W and asymmetric vibration of W-O_e-W (t, terminal; c, corner-sharing; e, edge-sharing),[22] respectively. These W-O stretching bands can be clearly observed in the corresponding FT-IR spectra of Mg_3Al-ILs-$La(PW_{11})_2$ and Mg_3Al-$La(PW_{11})_2$. Taking Mg_3Al-ILs-$La(PW_{11})_2$ as an example, the W-O stretching vibrations gave peaks located at 1089, 954, 889 and 775 cm^{-1}, respectively, which are slightly shifted due to the strong electrostatic interactions and hydrogen bonding between the host layers and intercalated POMs.[23] Moreover, the peak at 1051 cm^{-1} can be assigned to the stretching vibration of the P-O bond, which appears at 1046 cm^{-1} in the spectrum of $La(PW_{11})_2$. The FT-IR spectrum of Mg_3Al-ILs-$La(PW_{11})_2$ also exhibits new C-H stretching vibrations at 2930 and 2856 cm^{-1} due to the alkyl chain -CH_2 and -CH_3 groups, while the C=N stretching appears at 1658 cm^{-1} originating from the imidazole ring of ILs, respectively. Additionally, the peak located at 448 cm^{-1} is assigned to the O-M-O (M = Mg or Al) vibration of the brucite-like layers of the LDHs.[24]

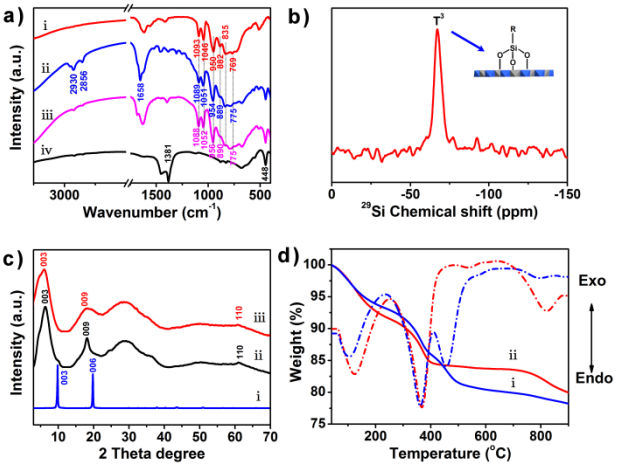

Figure 1. a) FT-IR spectra of (i) $La(PW_{11})_2$, (ii) Mg_3Al-ILs-$La(PW_{11})_2$, (iii) Mg_3Al-$La(PW_{11})_2$, (iv) Mg_3Al-NO_3; b) The ^{29}Si CP/MAS NMR spectrum of Mg_3Al-ILs-$La(PW_{11})_2$ and inset picture shows the structure model of T^3; c) XRD patterns of (i) Mg_3Al-NO_3; (ii) Mg_3Al-$La(PW_{11})_2$, (iii) Mg_3Al-ILs-$La(PW_{11})_2$; d) TG-DTA profiles of (i) Mg_3Al-ILs-$La(PW_{11})_2$ and (ii) Mg_3Al-$La(PW_{11})_2$.

It should be noted that the stretching band at 1384 cm^{-1} for Mg_3Al-NO_3 due to the N-O vibration[25] of NO_3^- appears to be weak in the corresponding FT-IR spectra of Mg_3Al-ILs-$La(PW_{11})_2$ and Mg_3Al-$La(PW_{11})_2$, indicating almost quantitative exchange of NO_3^- by POM clusters. The above observations demonstrate that the ILs are grafted onto the layers of LDHs and the $La(PW_{11})_2$ clusters are intercalated into LDHs successfully. The FT-IR spectra of PW_{12}, P_2W_{18}, Mg_3Al-ILs-PW_{12}, Mg_3Al-ILs-P_2W_{18} are shown in Fig. S1.

Additional confirmation of the catalysts' composition and structural features was provided by the (CP/MAS) NMR studies. As shown in Fig. 1b, the solid-state ^{29}Si cross-polarization magic-angle spinning (CP/MAS) NMR spectrum of Mg_3Al-ILs-$La(PW_{11})_2$ exhibits a resonance peak centred at -66.4 ppm, which corresponds to T^3 [$Si(OM)_3$].[26] The presence of T^3 signal indicates there are M-O-Si bonds around Si atom (M = Mg or Al). These results confirm that the ILs are tethered onto the layers of LDHs covalently, resulting in the formation of Mg-O-Si and/or Al-O-Si within the interlayer space.

As shown in Fig. 1c, the XRD pattern of Mg_3Al-NO_3 exhibit a reflection peak centered at 2θ = 9.88, which is attributed to the characteristic reflection of basal plane (003) and corresponds to a spacing value of d_{003} = 0.89 nm. After the intercalation of the $La(PW_{11})_2$ anions, a shift of the (003) reflection to lower angles was observed (2θ = 6.28). This change corresponds to a basal spacing value of d_{003}=1.42 nm, indicating an increase of the interlayer region due to the intercalation of the $La(PW_{11})_2$ species in Mg_3Al-ILs-$La(PW_{11})_2$. The height of the interlayer region value of 0.94 nm was calculated by subtracting the dimensions of the host layer (0.48 nm) from the value of the d_{003} spacing (1.42 nm) of the Mg_3Al-ILs-$La(PW_{11})_2$ composite. The obtained value is in good agreement with the width of the POM cluster (with dimensions of just below 1 nm). This indicates that the $La(PW_{11})_2$ anion's "long axis" is oriented parallel in the interlayer region of the LDHs .

The TG-DTA of Mg_3Al-$La(PW_{11})_2$ (Fig. 1d) exhibits three-stage weight losses, where the first one takes place within the range of 25 to 250 ^oC and is attributed to the loss of water molecules adsorbed on the surface and interlayer region; the second weight loss can be attributed to the collapse of the layered structure of LDHs and the third weight loss corresponds to the decomposition of $La(PW_{11})_2$. In the case of Mg_3Al-ILs-$La(PW_{11})_2$, three main weight-loss stages can be observed, in which the first weight loss of 6.46 % between 25 and 240 ^oC can be ascribed to the removal of water molecules; the second weight loss of 13.10 % takes place between 240 and 650 ^oC which corresponds to the collapse of the layered structure and decomposition of the ionic liquid and the third weight loss of 1.87 % between 650 and 900 ^oC is due to the decomposition of $La(PW_{11})_2$.

As shown in Fig. 2a, the photoelectron peaks of Mg, Al, C, O, N, P, La and W can be clearly identified from X-ray photoelectron spectroscopy (XPS). The XPS spectrum of W(4f) photoemission (Fig. 2b) consists of two peaks originating from the spin orbital splitting of the $W4f_{7/2}$ and $W4f_{5/2}$ at 35.1 eV and 37.1 eV, respectively, which can be ascribed to the W in the W-O bond configuration and typically observed for W^{6+}.[28] As shown in Fig. 2c, Mg_3Al-ILs-$La(PW_{11})_2$ exhibits typical type-IV adsorption isotherms, and H3 type hysteresis loops at higher relative pressure (P/P_0>0.5), indicating the presence of both interlayer and interparticle mesopores structure. The pore size

distribution calculated by the Barrett-Joyner-Halenda (BJH) method shows a peak centred at around 3.8 nm (Inset Fig. 2c). The Mg_3Al-ILs-La$(PW_{11})_2$ exhibits a Brunauer-Emmett-Teller (BET) surface area of 43.99 m^2/g with a total pore volume of 0.18 cm^3/g. The N_2 adsorption-desorption isotherm and the pore size distribution of Mg_3Al-La$(PW_{11})_2$ are shown in Fig. S5 while a comparison of their physicochemical properties is shown in Table S1.

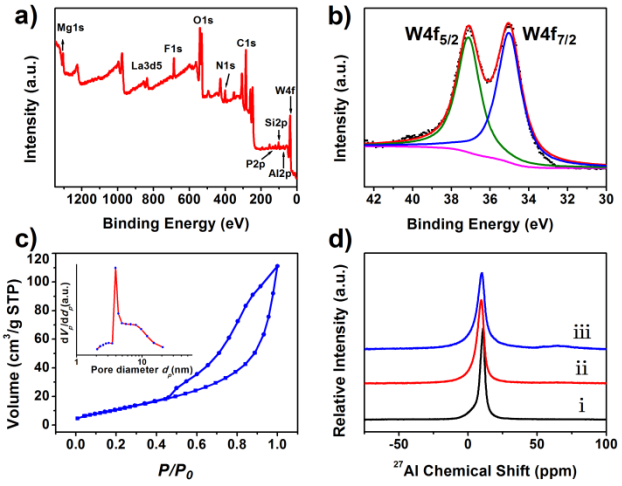

Figure 2. a) XPS survey spectrum of Mg_3Al-ILs-La$(PW_{11})_2$; b) XPS spectrum for the W_{4f} core level of Mg_3Al-ILs-La$(PW_{11})_2$; c) The N_2 adsorption-desorption isotherm and the pore size distribution (inset picture) of Mg_3Al-ILs-La$(PW_{11})_2$; d) The ^{27}Al-MAS-NMR spectra of (i) Mg_3Al-NO_3, (ii) Mg_3Al-La$(PW_{11})_2$, and (iii) Mg_3Al-ILs-La$(PW_{11})_2$.

The ^{27}Al resonance line positions are very sensitive to the coordination number and are expected to appear within the range of -5 to 15 ppm for the octahedral geometry of AlO_6 sites.[26] As shown in Fig. 2d, the solid state ^{27}Al-MAS-NMR spectrum of Mg_3Al-NO_3 exhibits a strong single signal at ~10.9 ppm, indicating the presence of octahedral geometry of AlO_6 sites in the brucite-like layers.[29-31] In the case of Mg_3Al-La$(PW_{11})_2$ and Mg_3Al-ILs-La$(PW_{11})_2$, the ^{27}Al-MAS-NMR signals are located almost at the same position (with a slight shift to low field chemical shift) in comparison to the Mg_3Al-NO_3. This observation indicates that the brucite-like layered structure retains its integrity upon intercalation of the POMs. Based on the TG-DTA, ICP and elemental analysis considerations, the formula of the composite material of Mg_3Al-ILs-La$(PW_{11})_2$ was identified as $Mg_{0.75}Al_{0.25}(OH)_{1.87}[O_3SiC_{14}H_{28}N_2]_{0.042}[PF_6]_{0.036}$ $[La(PW_{11}O_{39})_2]_{0.0225}\cdot 0.72H_2O$ (the POM loading, La$(PW_{11})_2$, found to be 104.56 μmol/g, W=42.3 wt. %, ILs= 5.9 wt.%).

Scanning Electron Microscopy studies of the composite material was used in order to obtain further information regarding the morphology of the catalyst in solid state. The SEM images of the as-prepared Mg_3Al-ILs-La$(PW_{11})_2$ (Fig. 3) showed uniform porous stacking of sheet-like crystallites with an average size of ~1 μm (Fig. 3a-c). The porous sheet-like morphology may be due to the high percentage of active coordinatively unsaturated atoms located at the edges on the crystallites.[32] Energy-dispersive spectroscopy (EDX) mapping (Fig. 3d) revealed the uniform dispersion of the composition element Mg, Al, C, O, W, which is closely related to the unique structural architecture of LDHs. In LDHs, the divalent (Mg^{2+}) and trivalent (Al^{3+}) cations can be highly dispersed within the brucite-like layers.[33] Moreover, the POMs are dispersed and orderly arranged in the two-dimensional (2D) confined gallery space. HRTEM images (Fig. 3e-g) and EDX results revealed the presence of highly dispersed black spots of 1.5 ~ 2 nm in diameter, which are in good agreement with the size of La$(PW_{11})_2$ clusters.

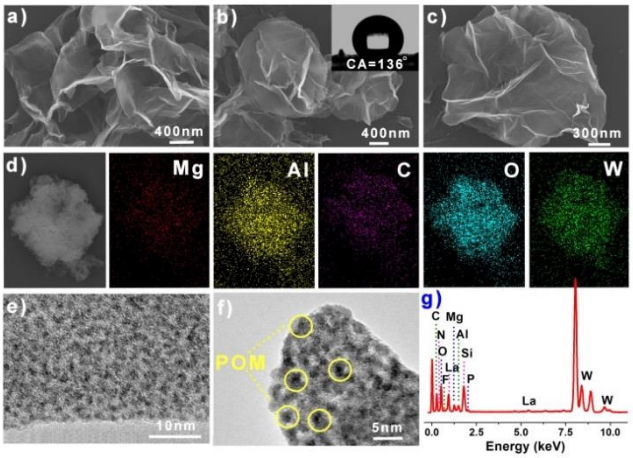

Figure 3. SEM images of a-c) Mg_3Al-ILs-La$(PW_{11})_2$, inset picture in image b shows the water contact angle measurements of Mg_3Al-ILs-La$(PW_{11})_2$, d) compositional EDX mapping of the Mg_3Al-ILs-La$(PW_{11})_2$; HRTEM images of e-f) Mg_3Al-ILs-La$(PW_{11})_2$ and g) its corresponding EDX.

In order to gain better understanding of the interactions between the catalyst and substrates under the employed experimental conditions, the amphiphilic property of the intercalated catalyst was investigated (inset picture in Fig. 3b). The LDH layers are hydrophilic due to the presence of numerous hydroxyl groups and water molecules in the interlayer galleries. However, when a water droplet contacts the sheet of Mg_3Al-ILs-La$(PW_{11})_2$, it forms a contact angle of 136°, indicating a moderate hydrophobicity and excellent surface wettability for the organic substrate. This observation suggests that the hydrophobicity of the intercalated catalyst is increased due to the modification of the LDHs layers with ionic liquids, leading finally to easier access and more effective interaction of the substrate with the catalytic site. Additional, SEM, HRTEM, EDX spectra of the Mg_3Al-ILs-PW_{12} and Mg_3Al-ILs-P_2W_{18} composites are reported in the ESI (Fig. S6).

Selective sulfoxidation of thioanisole

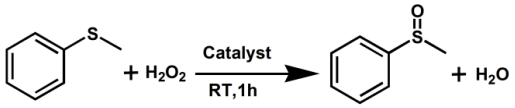

Scheme 1. Model reaction of selective oxidation of thioanisole.

Oxidative transformations of organic compounds under mild conditions are of great importance in industrial processes and synthetic organic chemistry.[34-35] The selective oxidation of sulfides to sulfoxides and sulfones is a pivotal reaction due to its use in chemical industry, medicinal chemistry and biology.[14] In this work, we aim at exploring the efficiency of different catalysts for selective oxidative of thioanisole in the presence of different substrates and H_2O_2 (Scheme 1). In order to evaluate the feasibility, we used thioanisole as a model substrate in the presence of H_2O_2 (30 %) as the oxidant for the model reaction.

Table 1. Selective oxidation of thioanisole in methanol with H_2O_2 by different catalysts.[a]

Entry	Catalyst	Conv[b] (%)	Selec[b] (%)
1	Mg_3Al-La$(PW_{11})_2$	80.5	91.3
2	Mg_3Al-ILs-La$(PW_{11})_2$	99.9	97.6
3	Mg_3Al-NO_3	25.4	98.6
4	ILs	73.6	98.2
5	Mg_3Al-NO_3+ILs+ La$(PW_{11})_2$	79.4	95.8
6	$Mg(OH)_2$	18.6	82.5
7	$Al(OH)_3$	17.8	83.4
8	None	17.3	82.5
9	Mg_3Al-ILs-PW_{12}	83.8	88.7
10	Mg_3Al- ILs-P_2W_{18}	81.7	91.7

[a] Reaction conditions: 1 mmol of thioanisole, 1 mmol of H_2O_2 (30 wt.%), 20 mg catalyst, T = 25 °C, t = 1 h. [b] Conversion and selectivity were determined by GC analysis using reference standards. Assignment of product was analysed by ^{1}H NMR and ^{13}C NMR in Fig. S7.

As shown in Table 1, the Mg_3Al-La$(PW_{11})_2$ shows 80.5 % conversion and 91.3 % selectivity (entry 1). Notably, the Mg_3Al-ILs-La$(PW_{11})_2$ exhibits excellent catalytic performance with 99.9 % conversion and 97.6 % selectivity (entry 2) under the same experimental conditions. However, only 17.3 % conversion of sulfoxidation is obtained in the absence of catalyst (entry 8). Moreover, the reaction proceeds sluggishly when physical mixture of the individual components of the composite material, or the parent LDH (Mg_3Al-NO_3), and/or ILs (entries 3-5) was used as catalysts. To prove that the catalytic activity is not the effect of potential impurities, we studied the efficiency of $Mg(OH)_2$ and $Al(OH)_3$ (entries 6 and 7) which revealed only 18.6 and 17.8 % conversion, respectively. The control experiments (entries 9-10) exhibits inferior catalytic activity in the case where other classical POMs such as Keggin (Mg_3Al-ILs-PW_{12}) and Well-Dawson (Mg_3Al-ILs-P_2W_{18}) were incorporated in the LDH. The results suggest that the Mg_3Al-ILs-La$(PW_{11})_2$ is one of the most efficient catalysts for sulfoxidation reactions.

The oxidation of organosulfur compounds involves an electrophilic attack of an activated peroxo species to the sulfide.[36] The catalytic activity for such sulfoxidation is supposed to increase as a function of the electron deficiency on the catalytic active center.[15] Our previous work have demonstrated that grafting of ionic liquids onto LDHs nanosheets enhances the mass transfer in solid-liquid interface by improving the accessibility of the substrates to the active species.[21] Therefore, the above experimental results account for the observed difference of the catalytic activity when we use different catalysts. In addition, these results strongly support the importance of the synergistic effect between the components of the heterogeneous catalyst Mg_3Al-ILs-La$(PW_{11})_2$, which is reflected in the enhancement of the overall catalytic performance.

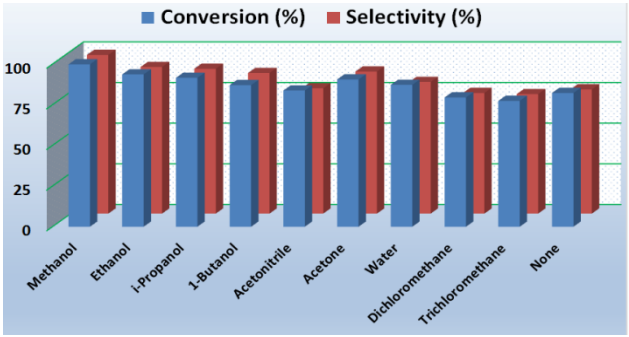

Figure 4. Effect of solvents on sulfoxidation of thioanisole by Mg_3Al-ILs-La$(PW_{11})_2$. Reaction conditions: 1 mmol of substrate, 1 mmol of H_2O_2 (30 wt. %), 20 mg catalyst, 200 μL of solvent, 25 °C, 1 h.

A series of solvents have been tried to investigate their effect on the catalytic activity, and the results showed a conversion of 99.9%, 93.7%, 91.6%, 87.1%, 83.8%, 90.6%, 87.3%, 79.5%, 77.4%, 82.3% for methanol, ethanol, *i*-propanol, 1-butanol, acetonitrile, acetone, water, dichloromethane, trichloromethane and solvent-free conditions, respectively (Fig. 4). The observed difference can be attributed to solvation effects and different interactions between thioanisole and the solvents. As a result, the optimized solvent for such a sulfoxidation reaction is methanol.

Kinetic study of sulfoxidation of thioanisole

In an effort to obtain the kinetic parameters for the model reaction, parallel experiments have been carried out under the optimized conditions. Taking the Mg_3Al-ILs-La$(PW_{11})_2$ as an example, the reaction proceeds smoothly at room temperature. Conversion and $\ln(C_t/C_0)$ are plotted against reaction time in Fig. 5, where C_0 and C_t are the initial thioanisole concentration and the concentration of thioanisole at time t, respectively. The

Mg_3Al-ILs-La$(PW_{11})_2$ exhibits excellent catalytic activity and the conversion can reach 99 % with above 97 % selectivity of the corresponding sulfoxide in 1 h. The linear fit of the data reveals that the catalytic reaction follows pseudo-first-order kinetics for selective oxidation of thioanisole reaction (R^2 = 0.992). The observed rate constant *k* for the selective oxidation reaction was determined to be 0.069 min^{-1} on the basis of Eqs. (1) and (2). Thus, the catalyst exhibits high catalytic efficiency for the sulfoxidation reaction, and the catalytic reaction obeys pseudo-first-order kinetics with > 97 % selectivity of the corresponding sulfoxide at a production rate of 208 mmol g^{-1} h^{-1} (mmol product produced per gram of catalyst per hour).

$$\frac{-dC_t}{dt} = kC_t \quad (1)$$

$$\ln\frac{C_0}{C_t} = kt \quad (2)$$

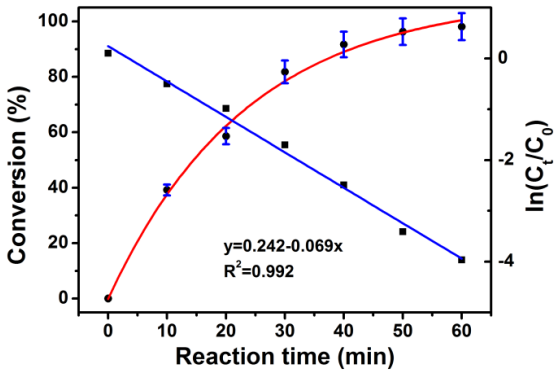

Figure 5. Kinetic profiles of oxidation of thioanisole under the optimized conditions; Reaction conditions: 1 mmol of thioanisole, 1 mmol of H_2O_2 (30 wt.%), 20 mg catalyst, 200 μL methanol, T = 25 ^oC.

In order to evaluate the applicability of the heterogeneous catalyst Mg_3Al-ILs-La$(PW_{11})_2$, a number of thioether-based compounds were used as substrates under the optimized reaction conditions (Table 2). The results demonstrate that we can achieve excellent conversion and selectivity for most thioethers (entries 1-9, 11). However, the benzyl phenyl sulfide showed relatively low conversion and poor selectivity, which might be attributed to the increased steric hindrance (entry 10). When the substrate/H_2O_2 molar ratio is 1:2, all the substrates can be selectively oxidized to the corresponding sulfone with excellent selectivity (Table S2).

Efficiency for selective oxidation of thioanisole to sulfoxides

The catalytic selective oxidation of sulfides using various catalysts that have been reported in the literature is summarized in Table 3. For example, Wang *et al*. reported a novel ionic liquid-based polyoxometalate (POM) catalytic system that shows exclusive oxidation of sulfoxide at room temperature at a very short time.[37] However, it should be noted that some of these reported catalytic systems suffer from low activity, hydrolytic and thermal stability under oxidative conditions, catalyst leaching, recycling issues, *etc*.

Table 2. Selective oxidation of various sulfides to sulfoxides catalyzed by Mg_3Al-ILs-La$(PW_{11})_2$ in methanol.[a]

Entry	Substrate	Product	*T* (h)	Conv [b] (%)	Selec[b] (%)
1			1	99	98
2			1	95	95
3			1	99	99
4		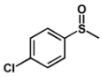	2	95	97
5		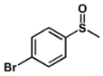	2	94	95
6	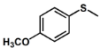	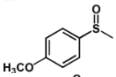	2	96	99
7		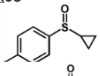	2	93	94
8	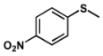		6	87	99
9		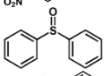	3	83	85
10	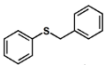	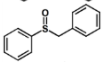	4	30	35
11	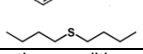	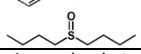	4	90	91

[a] Reaction conditions: 1 mmol substrate, 1 mmol of H_2O_2 (30 wt.%), 20 mg catalyst, T = 25 ^oC. [b] Conversion and selectivity were determined by GC analysis using reference standards.

Another important factor is the high cost of some catalytic systems which renders them unsuitable candidates for large scale experiments or industrial applications. In contrast, the sulfoxidation of thioanisole using Mg_3Al-ILs-La$(PW_{11})_2$ exhibits high efficiency and selectivity, along with excellent stability, recyclability and very efficient use of H_2O_2 (Substrate:H_2O_2 = 1:1) during the catalytic cycles (Table 2 and Table 3, entry 13), which renders it an ideal candidate for large scale experiments.

Table 3. Oxidation of thioanisole to sulfoxides by different catalysts with H_2O_2 as oxidant.

Entry	Catalyst	H_2O_2 (equiv.)	T.(^oC)	Time (h)	Conv. (%)	Sel.of sulfoxide	Ref
1	WO_3/MCM-48	1.1	rt	4	95	97	38
2	TiO_2	1.2	80	3	100	0.5	39

3	$(TBA)_2[SeO_4\{WO(O_2)_2\}_2]$	1	20	2	99	90	40
4	$(TBA)_4[\gamma\text{-}SiW_{10}O_{34}(H_2O)_2]$	0.2	32	1	98	99	41
5	Fe_3O_4@SiO_2APTES	3	rt	1.5	96	95	42
6	WO_4^{2-}/silica-NH_3^+	3	rt	1.5	82	100	43
7	BisILs-C_8H_{17}-$[W_2O_3(O_2)_4]$	1.1	rt	1.5	98.6	-	44
8	DA-La$(PW_{11})_2$	1	25	6	91	99	45
9	$[C4mim]_2$HPM	1.1	25	0.5	98.8	98.4	37
10	$[PO_4[WO(O_2)_2]_4]$@PIILP	2.5	rt	0.25	95	96	46
11	Ti-IEZ-MWW	1	rt	2	99	94	47
12	Mg_3Al-P_2W_{17}Zn	1	rt	6	96	100	15
13	Mg_3Al-ILs-La$(PW_{11})_2$	1	25	1	99	98	This work

Epoxidation of olefin

The efficiency of the Mg_3Al-ILs-La$(PW_{11})_2$ composite was further evaluated in olefin epoxidation reactions (Fig. 6). In an effort to identify the optimized epoxidation reaction conditions, a series of solvents, concentration and the substrate/H_2O_2 molar ratios were carefully explored (Fig. S 9-10). The optimum conditions are: *cis*-cyclooctene 1 mmol, H_2O_2 3 mmol, 1 ml CH_3CN, 40 mg catalyst. We investigated the effect of reaction time on the epoxidation of *cis*-cyclooctene by Mg_3Al-ILs-La$(PW_{11})_2$. The reaction conversion increases as a function of the reaction time. However, when the reaction temperature reaches to 70 °C, the reaction conversion does not increase anymore. Thus, the experiments to determine the kinetic parameters for the epoxidation of *cis*-cyclooctene were carried out at 70 °C.

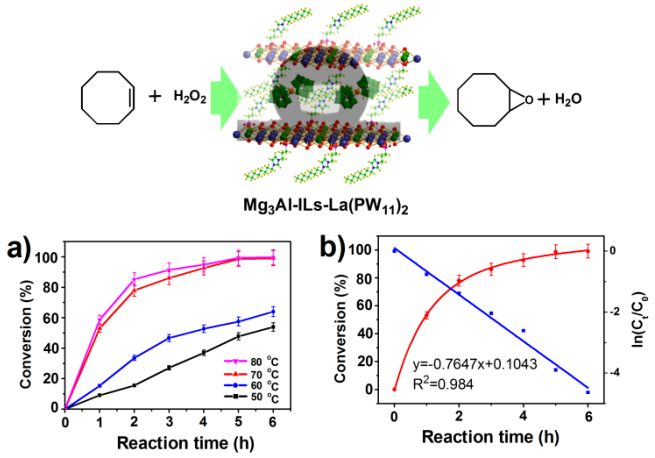

Figure 6. Top: schematic diagram of the catalytic epoxidation of *cis*-cyclooctene. a) Effect of reaction time on epoxidation of *cis*-cyclooctene by Mg_3Al-ILs-La$(PW_{11})_2$ under different temperatures b) Kinetic profiles of the epoxidation reaction. Reaction conditions: 1 mmol of substrate, 3 mmol H_2O_2 (30 wt. %), 40 mg catalyst, 1 ml CH_3CN; T = 70 °C.

Conversion and ln(C_t/C_0) are plotted against reaction time in Fig. 6b, where C_0 and C_t are the initial *cis*-cyclooctene concentration and *cis*-cyclooctene concentration at time t, respectively. The linear fit of the data reveals that the catalytic reaction shows pseudo-first-order kinetics for the epoxidation reaction (R^2 = 0.984). The observed rate constant k was determined to be 0.7647 h^{-1} on the basis of Eqs. (1) and (2). The Mg_3Al-ILs-La$(PW_{11})_2$ shows pretty good catalytic activity producing 31 mmol g^{-1} h^{-1} (mmol product produced per gram of catalyst per hour) of oxidation product while the conversion and selectivity reached a value of 99 % in 5 h.

The Mg_3Al-ILs-La$(PW_{11})_2$ exhibited high conversion and selectivity (Table 4) in the epoxidation of other well-known olefins such as cyclohexene and cyclododecene (entries 2-3). Moreover, the catalyst can be applied to the epoxidation of allylic alcohols (*trans*-2-hexene-1-ol) with 93 % conversion and 95 % selectivity (entry 4). The catalytic efficiency of previously reported systems for the epoxidation of olefin substrates are summarized in Table S3 (see the Supporting Information). The results confirm that the Mg_3Al-ILs-La$(PW_{11})_2$ is an excellent heterogeneous catalyst for the epoxidation of olefins.

Table 4. The epoxidation of various substrates over catalyst Mg_3Al-ILs-La$(PW_{11})_2$.[a]

Entry	Substrates	Time (h)	Conv[b] (%)	Selec[b] (%)
1	*cis*-cyclooctene	5	97	99
2	cyclohexene	5	96	99
3	cyclododecene	12	82	99
4	*trans*-2-hexene-1-ol	2	93	95

[a]Epoxidation of different substrates with H_2O_2 catalyzed with Mg_3Al-ILs-La$(PW_{11})_2$. Reaction conditions: 1 mmol of substrate, 40 mg catalyst, 3 mmol H_2O_2 (30 wt.%), 1 ml CH_3CN; T = 70 °C. [b] Conversion and selectivity were determined by GC analysis using reference standards.

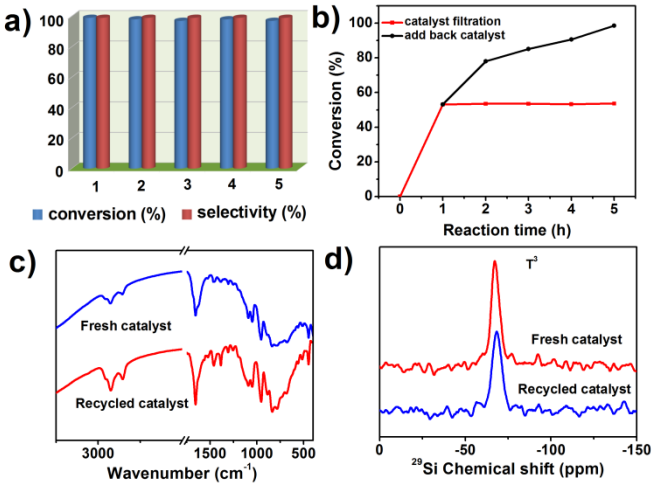

Figure 7. a) Catalytic reusability of Mg_3Al-ILs-La$(PW_{11})_2$ for sulfoxidation of thioanisole; b) Experiment to prove the nature of heterogeneous catalyst; c)

FT-IR spectra and d) solid-state ^{29}Si CP/MAS NMR spectra of the fresh and used Mg_3Al-ILs-La$(PW_{11})_2$.

The catalyst's stability and recyclability are essential requirements for larger scale applications.[48-49] In order to evaluate the recyclability of the catalytic system, we repeated the selective oxidation of thioanisole using Mg_3Al-ILs-La$(PW_{11})_2$. The catalyst was separated from the reaction mixture by centrifugation, washed with acetone, dried and re-used by addition of fresh substrate and H_2O_2 (30 wt. %) at 25 ^oC (Fig. 7a). During the five-run recycling test, the conversion found to be 99.9 %, 98.2 %, 98.4 %, 97.8 %, 97.5 %, 97.1 %, while the selectivity remains above 98 %. Inductively coupled plasma atomic emission analysis (ICP-AES) of the recycled catalyst confirms that the polyoxometalate is stable by intercalating into the 2D confined space of LDHs. Moreover, the tungsten content of 41.2 wt.% for the recycled catalyst is close to that of the fresh catalyst (42.3 wt.%), indicating the absence of leaching issues.

When the epoxidation reaction was half-way through (after 1h the conversion reached a value of 52 %), the Mg_3Al-ILs-La$(PW_{11})_2$ was removed by filtration. The remaining reaction mixture kept under the same experimental conditions in the absence of the catalyst for 4h. Analysis of the reaction mixture revealed that no additional oxidation product was detected (Fig. 7b, red line). As soon as the solid Mg_3Al-ILs-La$(PW_{11})_2$ was added back to the reaction mixture, the catalytic reaction resumed as expected.(Fig. 7b, black line). The experiment demonstrates that the Mg_3Al-ILs-La$(PW_{11})_2$ is a truly efficient and robust heterogeneous catalyst. FT-IR (Fig. 7c), solid-state ^{29}Si cross-polarization magic-angle spinning (CP/MAS) NMR (Fig. 7d) and XPS spectra for the W_{4f} core level (Fig. S12), as well as the SEM, HRTEM images and EDX of the recycled Mg_3Al-ILs-La$(PW_{11})_2$ (Fig. S13) suggest that the catalyst retains its morphology and structural integrity.

In order to evaluate the potential of the heterogeneous catalyst, we have focused our attention on the gram-scale synthesis of sulfoxide and epoxides. We have performed the selective oxidation of thioanisole and epoxidation of *cis*-cyclooctene reaction by scaling up the amount of substrate by a factor of 50. The scaled-up experiment reactions proceeded smoothly under the optimized experimental conditions. Using the selective oxidation of thioanisole as an example, we obtained excellent yields of the corresponding sulfoxides (96 %) with 99% selectivity under the optimized experimental conditions of 50 mmol thioanisole, 50 mmol H_2O_2, 10 ml CH_3OH, 1 g Mg_3Al-ILs-La$(PW_{11})_2$, at 25 ^oC and 1h reaction time. The results demonstrate the potential of the designed heterogeneous catalyst for industrial applications.

Conclusions

In summary, a multicomponent heterogeneous catalyst Mg_3Al-ILs-La$(PW_{11})_2$ was synthesized by adopting an exfoliation/assembly approach. The grafting of ILs on the LDH not only induces flexibility to the catalyst but also allows easy access of the substrates to the active centre. The resultant catalyst shows high efficiency in the catalysis of various substrates such as the selective sulfoxidation of sulfides to sulfoxide, sulfones and epoxidation of olefins under mild conditions. The catalyst of Mg_3Al-ILs-La$(PW_{11})_2$ can promote efficiently sulfoxidation reactions at 25 ^oC in 60 min with the conversion and selectivity remaining above 99 and 98 % respectively, producing 208 mmol g^{-1} h^{-1} of oxidation product. Additionally, it also can promote efficiently the epoxidation of *cis*-cyclooctene at 70 ^oC in 5 h with the conversion and selectivity remaining above 97 and 99 % respectively, generating 31 mmol g^{-1} h^{-1} of epoxides. Moreover, the structural stability of the Mg_3Al-ILs-La$(PW_{11})_2$ composite is retained during the re-cycling process due to the multiple interactions between the three components (host layers, ILs and POMs). The Mg_3Al-ILs-La$(PW_{11})_2$ composite can be separated easily from the reaction mixture by simple filtration and recycled at least five times without obvious decrease of its catalytic activity. Finally, the scaled-up experiment demonstrated the potential of the heterogeneous catalyst for industrial applications.

Experimental Section

Chemical Materials

All chemicals were of analytical grade and were used as received without any further purification. The $K_{11}[La(PW_{11}O_{39})_2]\cdot 13H_2O$ [$La(PW_{11})_2$],[50] $Na_3PW_{12}O_{40}\cdot 15H_2O$ (PW_{12}),[51] $K_6[P_2W_{18}O_{62}]\cdot 14H_2O$ (P_2W_{18}),[52] $[Mg_{0.75}Al_{0.25}(OH)_2](CO_3)_{0.125}\cdot 2H_2O$ (Mg_3Al-CO_3),[53] $[Mg_{0.75}Al_{0.25}(OH)_2](NO_3)_{0.25}\cdot 2H_2O$ (Mg_3Al-NO_3),[54] 1-octyl-3-(3-triethoxy-silylpropyl)-4,5-dihydro-imidazolium hexafluorophosphate (ILs),[55] Mg_3Al-ILs[21] were synthesized according to previously reported literature procedures.

Synthesis of Mg_3Al-ILs-La$(PW_{11})_2$

Mg_3Al-NO_3 (0.3 g) was added into 300 mL of formamide in a three-necked flask purged with N_2. The mixture was vigorously stirred for 2 days. Then, the mixture was centrifuged for 10 min and the suspension was separated simply by filtration. Then, ILs (2.6 mmol) was dissolved in CH_3CN/CH_2Cl_2 (1:1, 5 mL) and added dropwise to the above isolated suspension. The reaction mixture was stirred under N_2 for 24 hours. The $K_{11}[La(PW_{11}O_{39})_2]\cdot 13H_2O$ (1.68 g, $La(PW_{11})_2$) was dissolved in 30 mL formamide and added dropwise to the above solution. The precipitate of Mg_3Al-ILs-La$(PW_{11})_2$ (1.0 g) was collected by filtration and washed with ethanol, water and dried under vacuum overnight. Mg_3Al-ILs-PW_{12} and Mg_3Al-ILs-P_2W_{18} were obtained using similar procedure.

Catalytic test

In a typical sulfide oxidation experiment, a mixture of 1 mmol thioanisole, 1 mmol H_2O_2 (30 wt. %), 200 μL CH_3OH and 20 mg catalyst Mg_3Al-ILs-La$(PW_{11})_2$ (2.1 μmol based on $La(PW_{11})_2$) were added into a 10 mL glass bottle and the reaction mixture was kept under stirring at 25 ^oC. In a typical olefin epoxidation experiment, a mixture of 1 mmol

cis-cyclooctene, 3 mmol H_2O_2 (30 wt. %), 1 mL CH_3CN and 40 mg catalyst Mg_3Al-ILs-La$(PW_{11})_2$ (4.2 μmol based on La$(PW_{11})_2$) were added into a 10 mL glass bottle and the reaction mixture was kept under vigorous stirring at 70 °C. The resulting products were extracted with diethyl ether, analysed by GC and identified by ^{1}H-NMR and ^{13}C-NMR in order to determine the selectivity and conversion.

Acknowledgements

This research was supported by the National Basic Research Program of China (973 program, 2014CB932104), National Nature Science Foundation of China (U1407127, U1507102, 21521005, 21625101), International Joint Graduate-Training Program of Beijing University of Chemical Technology, and Fundamental Research Funds for the Central Universities (ZY1709). H. N. M. acknowledges the financial support from the University of Glasgow.

Keywords: Polyoxometalates • Layered double hydroxides • sulfoxidation • epoxidation • heterogeneous catalyst

[1] S. S. Wang, G. Y. Yang, *Chem. Rev*. **2015**, *115*, 4893-4962.

[2] Y. Zhou, G. Q. Chen, Z. Y. Long, J. Wang, *RSC Adv*. **2014**, *4*, 42092-42113.

[3] H. N. Miras, L. Vilà-Nadal, L. Cronin, *Chem. Soc. Rev*. **2014**, *43*, 5679-5699.

[4] R. Kawahara, S. Uchida, N. Mizuno, *Chem. Mater*. **2015**, *27*, 2092-2099.

[5] a) M. Lechner, R. Güttel, C. Streb, *Dalton Trans.,* **2016**, *45*, 16716-16726; b) C. Chen, H. Yuan, H. F. Wang, Y. F. Yao, W. B. Ma, J. Z. Chen, Z. S. Hou, *ACS Catal*. **2016**, *6*, 3354-3364.

[6] J. Li, D. F. Li, J. Y. Xie, Y. Q. Liu, Z. J. Guo, Q. Wang, Y. O. Lyu, Y. Zhou, J. Wang, *J. Catal*. **2016**, *339*, 123-134.

[7] J. Z. Chen, L. Hua, W. W. Zhu, R. Zhang, L. Guo, C. Chen, H. M. Gan, B. N. Song, Z. S. Hou, *Catal. Commun*. **2014**, *47*, 18-21.

[8] F. Y. Song, Y. Ding, B. C. Ma, C. M. Wang, Q. Wang, X. Q. Du, S. Fu, J. Song, *Energy. Environ. Sci*. **2013**, *6*, 1170-1184.

[9] S. Omwoma, W. Chen, R. Tsunashima, Y. F. Song, *Coord. Chem. Rev*. **2014**, *258-259*, 58-71.

[10] Y. Zhou, Z. J. Guo, W. Hou, Q. Wang, J. Wang, *Catal. Sci. Technol.* **2015**, *5*, 4324-4335.

[11] K. Yamaguchi, C. Yoshida, S. Uchida, N. Mizuno, *J. Am. Chem. Soc*. **2005**, *127*, 530-531.

[12] B. Karimi, M. Khorasani, *ACS Catal*. **2013**, *3*, 1657-1664.

[13] E. Poli, R. D. Sousa, F. Jerome, Y. Pouilloux, J. M. Clacens, *Catal. Sci. Technol*. **2012**, *2*, 910-914.

[14] L. L. Hong, P. Win, X. Zhang, W. Chen, H. N. Miras, Y. F. Song, *Chem. Eur. J*. **2016**, *22*, 11232-11238.

[15] K. Liu, Z. X. Yao, Y. F. Song, *Ind. Eng. Chem. Res*. **2015**, *54*, 9133-9141.

[16] G. L. Fan, F. Li, D. G. Evans, X. Duan, *Chem. Soc. Rev*. **2014**, *43*, 7040-7066.

[17] R. Y. Yang, Y. S. Gao, J. Y. Wang, Q. Wang, *Dalton Trans*. **2014**, *43*, 10317-10327.

[18] Y. Q. Jia, Y. J. Fang, Y. K. Zhang, H. N. Miras, Y. F. Song, *Chem. Eur. J*. **2015**, *21*, 14862-14870.

[19] Y. Leng, J. W. Zhao, P. P. Jiang, J. Wang, *ACS Appl. Mater. Inter*. **2014**, *6*, 5947-5954.

[20] a) S. Herrmann, A. Seliverstov, C. Streb, *J. Molec. Engin. Mater*. **2014**, *2*, 1440001-1440007; b) S. Herrmann, L. D. Matteis, J. M. de la Fuente, S. G. Mitchell, C. Streb, *Angew. Chem. Int. Ed.* **2017**, *56*, 1667-1670; c) S. Herrmann, M. Kostrzewa, A. Wierschem, and C. Streb, *Angew. Chem. Int. Ed*. **2014**, *53*, 13596-13599.

[21] T. F. Li, Z. L. Wang, W. Chen, H. N. Miras, Y. F. Song, *Chem. Eur. J*. **2017**, *23*, 1069-1077.

[22] K. Liu, Z. X. Yao, H. N. Miras, Y. F. Song, *ChemCatChem*, **2015**, *7*, 3903-3910.

[23] Y. B. Dou, J. B. Han, T. L. Wang, M. Wei, D. G. Evans, X. Duan, *Langmuir*, **2012**, *28*, 9535-9542.

[24] Z. P. Xu, H. C. Zeng, *Chem. Mater*. **2001**, *13*, 4555-4563.

[25] G. L. Huang, S. L. Ma, X. H. Zhao, X. J. Yang, K. Ooi, *Chem. Mater*. **2010**, *22,* 1870-1877.

[26] A. Y. Park, H. Kwon, A. J. Woo, S. J. Kim, *Adv. Mater*. **2005**, *17*, 106-109.

[27] a) L. Li, R. Z. Ma, Y. Ebina, N. Iyi, T. Sasaki, *Chem. Mater*. **2005**, *17*, 4386-4391; b) S. Zhao, J. H. Xu, M. Wei, Y. F. Song, *Green Chem.,* **2011**, *13*, 384–389.

[28] L. Salvati, L. E. Makovsky, J. M. Stencel, F. R. Brown, D. M. Hercules, *J. Phys. Chem*. **1981**, *85*, 3700-3707.

[29] Y. Y. Liu, K. Murata, T. Hanaoka, M. Inaba, K. Sakanishi, *J. Catal*. **2007**, 248, 277-287.

[30] M. R. Weir, R. A. Kydd, *Inorg. Chem*. **1998**, *37*, 5619-5624.

[31] C. Venturello, R. D'Aloisio, J. J. Bart, M. Ricci, *J. Mol. Catal*. **1985**, *32*, 107-110.

[32] D. J. Liang, W. B. Yue, G. B. Sun, D. Zheng, K. Ooi, X. J. Yang, *Langmuir*, **2015**, *31*, 12464-12471.

[33] R. F. Xie, G. L. Fan, L. Yang, F. Li, *Chem. Eng. J*. **2016**, *288*, 169-178.

[34] Y. X. Qiao, Z. S. Hou, H. Li, Y. Hu, B. Feng, X. R. Wang, L. Hua, Q. F. Huang, *Green Chem.,* **2009**, *11*, 1955–1960.

[35] W. Zhao, C. Yang, Z. G. Cheng, Z. H. Zhang, *Green Chem*. **2016**, *18*, 995-998.

[36] H. Shi, C. Yu, J. He, *J. Phys. Chem. C*. **2010**, *114*, 17819-17828.

[37] P .P Zhao, M. J. Zhang, Y. J. Wu, J. Wang, *Ind. Eng. Chem. Res*. **2012**, *51*, 6641−6647.

[38] D. H. Koo, M. Kim, S. Chang, *Org Lett*. **2005**, *7*, 5015-5018.

[39] W. Al-Maksoud, S. Daniele, A. B. Sorokin, *Green Chem.* **2008**, *10*, 447-451.

[40] N. Mizuno, K. Kamata, K. Yamaguchi, *Top. Catal*. **2010**, *53*, 876-893.

[41] N. Mizuno, K. Yamaguchi, K. Kamata, *Catal. Surv. Asia*, **2011**, *15*, 68-79.

[42] A. Bayat, M. Shakourian-Fard, M. M. Hashemi, *Catal. Commun*. **2014**, *52*, 16-21.

[43] K. B, G. N. M, J. H. Clark, *Org. Lett*. **2005**, *7*, 625-628.
[44] X. Y Shi, X. Y Han, W. J Ma, J. F. Wei, J. Li, Q. Zhang, Z. G Chen, *J. Mol. Catal. A-Chem*. **2011**, *341*, 57-62.
[45] S. Zhao, Y. Q Jia, Y. F. Song, *Appl. Catal. A-Gen*. **2013**, *453*, 188–194.
[46] S. Doherty, J. G. Knight, M. A. Carroll, J. R. Ellision, S. J. Hobson, S. Stevens, C. Hardacre, P. Goodrich. *Green Chem*. **2015**, *17*, 1559-1571.
[47] Y. Kon, T. Yokoi, Masato Yoshioka, S. Tanaka, Y. Uesaka, T. Mochizuki, K. Sato, T. Tatsumi, *Tetrahedron*. **2014**, *70*, 7584-7592.
[48] X. C. Cai, Q. Wang, Y.Q. Liu, J. Y. Xie, Z. Y. Long, Y. Zhou, J. Wang, *ACS Sustain. Chem. Eng*. **2016**, *4*, 4986-4996.
[49] Z. J. Guo, X. C. Cai, J. Y. Xie, X. C. Wang, Y. Zhou, J. Wang, *ACS Appl. Mater. Inter*. **2016**, *8*, 12812-12821.
[50] R. D. Peacock, T. J. R. Weakley, J. Chem. Soc. A. **1971**, 1836-1839.
[51] N. Chen, R. T. Yang, *J. Catal*. **1995**, *157*, 76-86.
[52] C. R. Graham, R. G. Finke, *Inorg. Chem*. **2008**, *47*, 3679-3686.
[53] N. Iyi, Y. Ebina, T. Sasaki, *J. Mater. Chem*. **2011**, *21*, 8085-8095.
[54] Y. Q. Jia, S. Zhao, Y. F. Song, *Appl. Catal. A-Gen*. **2014**, *487*, 172-180.
[55] K. Yamaguchi, C. Yoshida, S. Uchida, N. Mizuno, *J. Am. Chem. Soc*. **2005**, *127*, 530-531.